

Host Galaxies of Long-Duration Gamma-Ray Bursts

Megan M. Bagley

University of Wyoming

mbagley@uwyo.edu

and

Lisa J. Kewley, Emily M. Levesque

Institute for Astronomy, University of Hawai'i

ABSTRACT

Long-duration gamma-ray bursts (GRBs) are associated with the deaths of massive, short-lived stars, and thus may be useful in tracking star formation in the universe. However, GRB progenitor models suggest that they might occur only in low-metallicity environments, introducing a bias into star formation studies. Presented here are the high-resolution spectra of two GRB host galaxies, one very nearby and one at $z \sim 0.7$. The nearby galaxy, the host of GRB 060218, has a low metallicity, but one that is comparable to local galaxies of similar luminosity. It has little to no extinction and a star formation rate of $\sim 2 \times 10^{-2} M_{\odot} \text{ yr}^{-1}$. The metallicity of the more distant galaxy, the host of GRB 991208, is not well constrained because the $\text{H}\alpha$ and $[\text{N II}]$ lines are redshifted into the near infrared and were not observed. It has a star formation rate of $1 - 9 M_{\odot} \text{ yr}^{-1}$ and, unlike the majority of GRB hosts, is dusty. These two galaxies will eventually be a part of a larger sample of GRB hosts.

Subject headings: gamma rays: bursts — galaxies: abundances — galaxies: fundamental parameters — galaxies: individual (GRB 991208, GRB 060218)

1. INTRODUCTION

The study of gamma-ray bursts (GRBs) and their progenitors has made much progress in recent years since the 2004 launch of the Swift satellite (Gehrels et al. 2004). Nevertheless, much still remains to be learned about the origin of these high-energy events.

GRBs are divided into two classes according to the duration of their gamma ray event: short hard bursts (< 2 s), and long soft bursts (> 2 s) (Kouveliotou et al. 1993). These two classes are produced by different mechanisms; from here on, we will focus on the long GRBs. Many long-duration GRBs have been observed simultaneously with Type Ibc supernovae, indicating that these

GRBs are produced in the explosive deaths of massive stars (e.g., Woosley & Bloom 2006). Only a small fraction of Type Ibc supernovae produce GRBs, however. GRB progenitor stars must have rapidly rotating inner cores at the end of their lifetimes, but mass loss and magnetic torques cause too much angular momentum loss in models (Woosley & Heger 2006). The rate of mass loss in Wolf-Rayet and O and B stars decreases with lower metallicity (Vink & de Koter 2005), so GRBs may preferentially occur in regions of low metallicity.

A GRB bias toward low-metallicity regions is supported by observations of GRB host galaxies. Stanek et al. (2006) and Modjaz et al. (2008) both found that GRB hosts lie offset from the luminosity-metallicity relation for star-forming galaxies; that is, GRB host galaxies are less metal-rich for a given luminosity than the general galaxy population. Indeed, GRB hosts have similar properties to extremely metal poor galaxies (Kewley et al. 2007): faint, blue, and generally smaller and more irregularly-shaped than the hosts of core-collapse supernovae that did not produce GRBs (Fruchter et al. 2006). Stanek et al. (2006) saw an inverse correlation between GRB energy and host galaxy metallicity, suggesting an upper metallicity limit for the formation of GRBs. High-redshift GRB hosts have high Lyman- α equivalent widths, usually found only in metal-poor systems (Fynbo et al. 2003).

On the other hand, Savaglio et al. (2008) found no clear indications that GRB host galaxies are different than normal star-forming galaxies. If GRBs are not biased toward low metallicity, they may be a powerful tool for tracing star formation through cosmic time because of their association with massive stars. Their young, blue stellar populations and high specific star formation rates are indicative of starbursting galaxies (Le Flocc’h et al. 2003).

What about the significant portion of star formation that has occurred in dusty, infrared-luminous galaxies? Many GRB hosts have low internal extinction, although some are relatively dusty (Kewley et al. 2007). One possibility is that only the GRBs with little extinction can be easily localized by their optical afterglow, and so the “dark bursts,” GRBs with no observed afterglows, represent the population of very dusty galaxies. The study of the hosts of these dark bursts is limited by lack of redshifts and other data. However, only a small fraction of GRB hosts, identified hosts of dark bursts included, are detected in the infrared (Le Flocc’h et al. 2006). Furthermore, GRBs are concentrated in the optically brightest regions of their host galaxies (Fruchter et al. 2006) rather than “hiding” in optically dark areas.

Only by further exploring the properties of GRB hosts can the questions of their metallicity and their use as star formation tracers be resolved. In this report, we examine two GRB hosts with high-resolution spectra and compare them to the galaxy population at large. Where applicable, we adopt $H_0 = 70 \text{ km s}^{-1} \text{ Mpc}^{-1}$.

2. SPECTRA

2.1. Observations

Three GRB host galaxies were observed on 01 June 2008 with the Low Resolution Imaging Spectrometer (LRIS) on the Keck I telescope at Mauna Kea. We used a $1.0'' \times 3.0'$ longslit with a 600/4000 grism, a 600/7500 grating, and a 560 dichroic. The first target, the host of GRB 030329, was not actually observed because our position reference, Gorosabel et al. (2005), gave a position that was ten seconds too high in R. A. The second target, the host of GRB 991208, was observed with the red side of LRIS, covering $6090 - 8710 \text{ \AA}$ to capture the rest-frame blue emission lines; the rest-frame red emission lines are redshifted to the near infrared. Six spectra of 1800 s each were taken. Our third target, the host of GRB 010921, was observed with both the blue and red sides of LRIS, giving a wavelength coverage of $5490 - 8110 \text{ \AA}$ to cover the rest-frame blue and red emission lines. Three spectra of 1800 s each were taken, but the signal-to-noise of the combined spectrum was too low to be useful, likely because of increasing sky noise as morning twilight approached.

In addition, the host galaxy of GRB 060218 was observed by Emily M. Levesque on 06 Sept 2007 with LRIS and the same settings as above except that a 900/5500 grating was used. Three spectra of 1800 s each were taken with both the blue and red sides of LRIS, covering $3050 - 5600 \text{ \AA}$ and $5320 - 7040 \text{ \AA}$ respectively, again capturing the rest-frame blue and red emission lines.

2.2. Data Reduction

The spectra were reduced using IRAF.¹ Reduction steps included subtracting the bias level using the *lrisbias* routine, trimming the spectra to remove the overscans and unilluminated parts of the chip, and dividing by a normalized flat. The individual two-dimensional spectra of each galaxy were then combined using a median combining operation in order to remove the effects of cosmic rays. One-dimensional spectra were extracted with the *apall* task, which also performed sky and background subtraction. These spectra were wavelength-calibrated with a Hg, Ne, Ar, Cd, and Zn arc taken immediately before or after the science images. Flux calibration of the GRB 991208 and GRB 060218 host spectra was done relative to the standard stars BD+33d2642 and EG 131, respectively.

The flux-calibrated spectra are shown in Figures 1 and 2.

¹IRAF is distributed by the National Optical Astronomy Observatories, which are operated by the Association of Universities for Research in Astronomy, Inc., under cooperative agreement with the National Science Foundation.

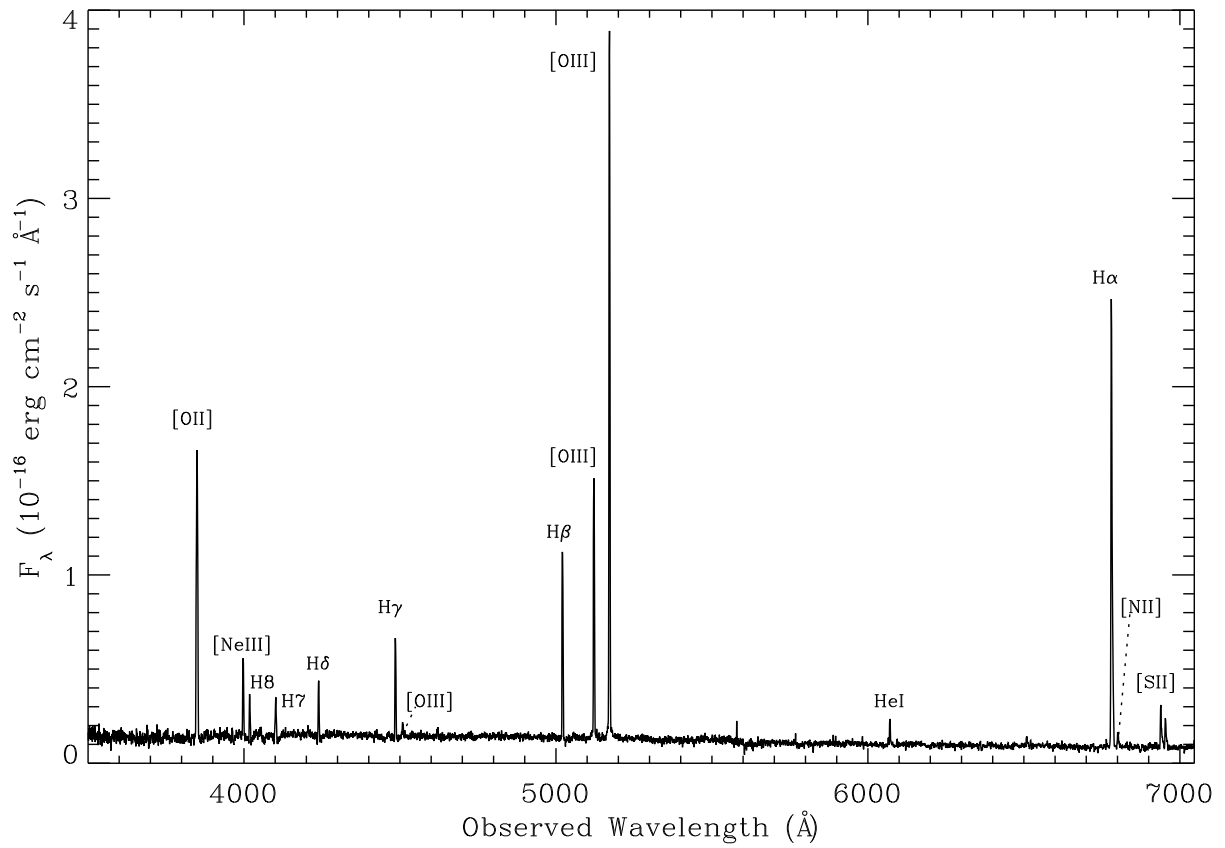


Fig. 1.— LRIS spectrum of the host galaxy of GRB 060218. Observed emission lines are labelled.

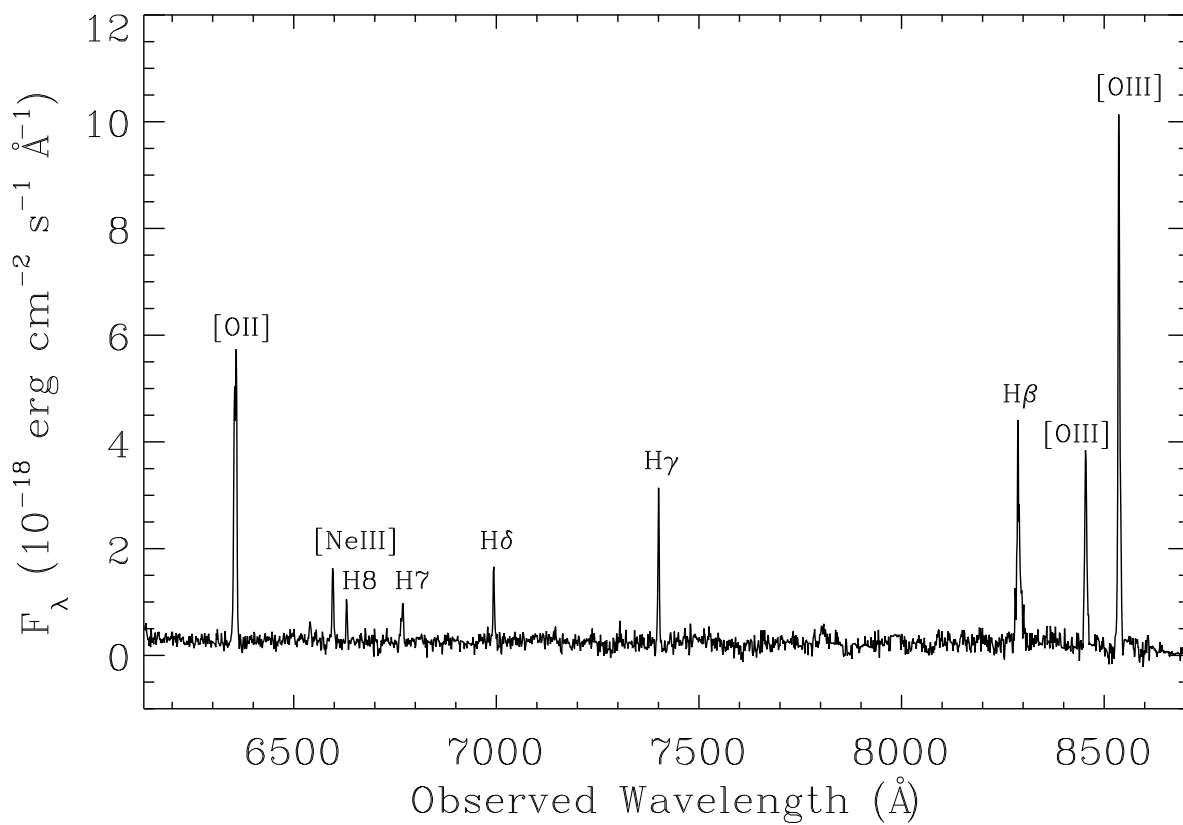


Fig. 2.— LRIS spectrum of the host galaxy of GRB 991208. Observed emission lines are labelled.

2.3. Emission Line Measurement

All emission lines were initially fit with a Gaussian using the IRAF task *splot*. Subsequent fits were done using *ngaussfit* on those lines for which the *splot* fit was poor. For the host of GRB 991208, the [O II] λ 3727 line was fit with two Gaussians in *splot* because the line had two distinct peaks, although not a clearly separable doublet. The H β and [O III] λ 5007 lines were fit with the sum of two Gaussians in *ngaussfit* because of their asymmetric shapes. For the host of GRB 060218, the H α and [S II] lines were also fit with the sum of two Gaussians because of their asymmetric shapes, while the H9, H8, H7, and H δ lines were fit with single Gaussians in *ngaussfit* to properly fit the absorption surrounding the lines.

The errors σ_l in the line fluxes were calculated with the formula of Pérez-Montero & Díaz (2003),

$$\sigma_l = \sigma_c \sqrt{N} \sqrt{\frac{1 + \text{EW}}{N\Delta}} \quad (1)$$

where σ_c is the RMS of the continuum around the line as measured in *splot*, Δ is the dispersion in Å per pixel, N is the number of pixels spanned by the line, and EW is the equivalent width of the line. This formula assumes Poissonian errors.

2.4. Reddening Correction

The emission-line fluxes were corrected for reddening using the observed Balmer lines and the Cardelli et al. (1989) reddening curve. The intrinsic Balmer line ratios were assumed to be those for Case B recombination at $T = 10^4$ K, $n_e = 10^2$ – 10^4 cm $^{-3}$ (Osterbrock 1989). A value of $R_V = A_V/E(B - V) = 3.1$ was assumed. After finding $E(B - V)$ for each galaxy, we dereddened the fluxes using the equation,

$$I_{true} = I_{observed} \times 10^{-0.4 k(\lambda)E(B-V)} \quad (2)$$

where $k(\lambda)$ is the wavelength-dependent constant from Cardelli et al. (1989).

The Balmer decrement of the host of GRB 060218 is 2.91, only slightly higher than the intrinsic ratio H α /H β = 2.86. The ratios H γ /H β and H δ /H β and the ratios of higher order Balmer lines relative to H β are all lower than and thus consistent with their intrinsic ratios. The galaxy was therefore assumed to have no reddening, i.e. $E(B - V) = 0.00$. To account for error, line fluxes with $E(B - V) = 0.05$ were also calculated.

Since H α was not observed for the host of GRB 991208, we use the H γ /H β and H δ /H β ratios to compute the extinction, finding $E(B - V) = 0.57$ – 0.60 . Fluxes for both the high and low values of reddening were calculated.

Table 1 gives the dereddened line fluxes and statistical errors for both GRB host galaxies.

Table 1. Dereddened Emission Line Fluxes

Line	$F(\lambda)/F(\text{H}\beta)$			
	GRB 060218		GRB 991208	
$E(B - V)$	0.00	0.05	0.57	0.60
$F(\text{H}\beta)^{\text{a}}$	4.24 ± 0.0825	5.00 ± 0.0974	2.26 ± 0.275	2.50 ± 0.304
3727 [O II]	2.009 ± 0.089	2.120 ± 0.094	2.359 ± 0.393	2.436 ± 0.406
3835 H9	0.075 ± 0.014	0.079 ± 0.015	0.094 ± 0.032	0.097 ± 0.032
3869 [Ne III]	0.382 ± 0.030	0.401 ± 0.032	0.341 ± 0.069	0.352 ± 0.072
3889 H8	0.224 ± 0.018	0.235 ± 0.019	0.150 ± 0.034	0.154 ± 0.035
3970 H7	0.292 ± 0.024	0.306 ± 0.025	0.231 ± 0.045	0.237 ± 0.046
4101 H δ	0.274 ± 0.019	0.285 ± 0.020	0.259 ± 0.057	0.265 ± 0.058
4340 H γ	0.471 ± 0.024	0.483 ± 0.024	0.463 ± 0.150	0.470 ± 0.152
4363 [O III]	0.097 ± 0.015	0.099 ± 0.015
4861 H β	1.000 ± 0.039	1.000 ± 0.039	1.000 ± 0.243	1.000 ± 0.243
4959 [O III]	1.373 ± 0.047	1.367 ± 0.047	0.677 ± 0.361	0.675 ± 0.360
5007 [O III]	3.401 ± 0.095	3.380 ± 0.094	1.561 ± 0.335	1.555 ± 0.334
5876 He I	0.113 ± 0.011	0.109 ± 0.010
6563 H α	2.915 ± 0.087	2.774 ± 0.083
6584 [N II]	0.086 ± 0.012	0.092 ± 0.013
6717 [S II]	0.263 ± 0.017	0.250 ± 0.016
6731 [S II]	0.155 ± 0.013	0.147 ± 0.012

^aIn units of 10^{-16} erg s $^{-1}$ cm $^{-2}$.

3. DERIVED QUANTITIES

3.1. Metallicity

3.1.1. GRB 060218

Because of the low redshift of the host of GRB 060218, the full complement of optical emission lines were observed. The temperature-sensitive [O III] λ 4363 line was detected, indicating a low metallicity. We derived the gas-phase oxygen abundance by several methods to facilitate comparison with other galaxies.

The [S II] λ 6717/[S II] λ 6731 line ratio gave an electron density n_e in the low-density limit, so n_e was assumed to be 20 cm^{-3} . The IRAF task *stdas.analysis.nebular.temden* computed the electron temperature based on a five-level atomic model (Shaw & Dufour 1994), giving an electron temperature of $1.8 \times 10^4 \text{ K}$. The oxygen abundance was computed using the electron temperature and the ratio of [O III] λ 4363 to [O III] λ 4959, 5007, following the procedure of Izotov et al. (2006), which is based on a classical two-zone H II region model. The resulting metallicity is $12+\log(\text{O}/\text{H}) \sim 7.58$ (the metallicities with $E(B-V) = 0.05$ are not significantly different given that the uncertainty in the metallicity calibration is $\sim 0.1 \text{ dex}$).

We also found the oxygen abundance using the strong-line calibrations of McGaugh (1991, hereafter M91) (as parameterized in Kobulnicky et al. 1999) and Kobulnicky & Kewley (2004, hereafter KK04). These calibrations are based on photoionization models of H II regions and employ the R_{23} parameter, the ratio of [O II] λ 3727 and [O III] λ 4959, 5007 to $\text{H}\beta$. The behavior of R_{23} with metallicity is double-valued, so we use the ratio of [N II] λ 6584 to [O II] to break the degeneracy. With $\log([\text{N II}]/[\text{O II}]) \sim -1.4$, the galaxy lies on the lower-metallicity branch of the R_{23} diagnostic, which also means that the [N II]/[O II] metallicity calibration of Kewley & Dopita (2002) cannot be directly used. The resulting M91 metallicity is ~ 7.98 (again, with $E(B-V) = 0.00$) and the KK04 metallicity is ~ 7.76 . The KK04 method includes calculation of the ionization parameter q . The very high ionization parameter of this galaxy, $8 \times 10^8 \text{ cm s}^{-1}$, results in the KK04 metallicity being lower than the M91 value, while the reverse is usually the case (Kewley & Ellison 2008). The uncertainty in these strong-line calibrations is $\sim 0.15 \text{ dex}$.

3.1.2. GRB 991208

No [O III] λ 4363 line was detected in the spectrum of the host of GRB 991208, so a T_e -based metallicity cannot be calculated. Without [N II] λ 6584 or $\text{H}\alpha$, which were redshifted into the near-infrared, the R_{23} methods are the only feasible options to calculate the metallicity, but it is very difficult to determine whether the galaxy lies on the high- or low-metallicity branch of the correlation. We therefore calculated possible high and low metallicities. The difference in metallicity for $E(B-V) = 0.57$ versus $E(B-V) = 0.60$ is negligible compared to the inherent error

in the calibrations; the following metallicities assume $E(B - V) = 0.60$. The upper-branch oxygen abundances are ~ 8.72 using the M91 calibration and ~ 9.07 using KK04, while the lower-branch values are ~ 7.85 using M91 and ~ 8.07 using KK04.

The derived properties of both galaxies are summarized in Table 2.

3.2. Star Formation Rate

The star formation rates (SFRs) were initially calculated using the standard SFR formulae of Kennicutt (1998). Using the $H\alpha$ line luminosity, the SFR of the host of GRB 060218 is $2.40 \times 10^{-2} M_{\odot} \text{ yr}^{-1}$ assuming $E(B - V) = 0.00$ as do the following numbers for this galaxy. Table 2 gives the SFR values for $E(B - V) = 0.05$, which are slightly higher. The dominant error in SFR is the uncertainty in $E(B - V)$.

The $[\text{O II}]\lambda 3727$ line luminosity is another SFR indicator, although less certain than $H\alpha$. Using $[\text{O II}]$, the SFR of the host of GRB 060218 is $2.92 \times 10^{-2} M_{\odot} \text{ yr}^{-1}$.

However, the classic SFR formulae frequently overestimate the SFR of low-metallicity galaxies (Kewley et al. 2007). We therefore recalculated the SFR of the host of GRB 060218 using the low-metallicity calibrations of Kewley et al. (2007) and Kewley et al. (2004), which use $H\alpha$ and $[\text{O II}]$ respectively. The first method gives a SFR of $1.19 - 1.25 \times 10^{-2} M_{\odot} \text{ yr}^{-1}$, depending on which value of metallicity is used. This value is approximately half the SFR found when metallicity is not considered. The second method, with $[\text{O II}]$, gives a an even lower SFR of $5.50 \times 10^{-3} M_{\odot} \text{ yr}^{-1}$.

Because the host of GRB 060218 is definitely a low-metallicity galaxy, we adopt the low-metallicity, $H\alpha$ -based SFR as the most accurate value, $\sim 1.2 \times 10^{-2} M_{\odot} \text{ yr}^{-1}$ assuming no extinction.

Since there is no measurement of the $H\alpha$ line for the host of GRB 991208, the SFR must be calculated from the $[\text{O II}]$ line luminosity. The SFR is very uncertain because the metallicity could be either high or low. Using the classic Kennicutt (1998) relation, the SFR is $8.18 M_{\odot} \text{ yr}^{-1}$ for $E(B - V) = 0.57$ and $9.33 M_{\odot} \text{ yr}^{-1}$ for $E(B - V) = 0.60$. By contrast, using Kewley et al. (2004) and assuming the galaxy has a lower-branch metallicity, the SFR is $1.62 M_{\odot} \text{ yr}^{-1}$ for $E(B - V) = 0.57$ and $1.86 M_{\odot} \text{ yr}^{-1}$ for $E(B - V) = 0.60$. Despite the uncertainty, it is evident that the host of GRB 991208 has an SFR about two orders of magnitude greater than does the host of GRB 060218.

3.3. Stellar Population Age

Although the age of the full underlying stellar population remains a mystery, one can calculate the age of the youngest stellar population on the basis of stellar population synthesis models. We use the models of Schaerer & Vacca (1998), assuming a Salpeter IMF and an instantaneous burst

of star formation, to convert the equivalent width of $H\beta$ to a stellar population age. The host of GRB 060218, with $EW(H\beta)=34.32 \text{ \AA}$, has an age of $6 - 8.7 \text{ Myr}$. The host of GRB 991208, with $EW(H\beta)=170.23 \text{ \AA}$, has an age of $2.4 - 4 \text{ Myr}$. The range of values in both cases depends on the exact choice of the absolute value of metallicity.

4. DISCUSSION

4.1. These Galaxies in the Literature

The host galaxy of GRB 060218 has been investigated by others largely because of the unusual properties of its GRB: a very long duration and soft emission (indeed, it is often classified as an X-ray flash). Wiersema et al. (2007), with a high resolution blue spectrum supplemented by a low resolution spectrum extending into the red, derived properties of this galaxy that agree with those presented here. Specifically, they report $E(B - V) \lesssim 0.03$ (no reddening within error), along with a very low electron density and high electron temperature. They calculated $12 + \log(O/H) \sim 7.54$ using the T_e method, equivalent to the 7.58 found with our LRIS spectrum. Similar metallicities were derived by Modjaz et al. (2008), who found ~ 7.5 with the T_e method, ~ 8.0 using the M91 calibration (comparable to this work’s 7.98 with no reddening), and ~ 8.1 by KK04 (somewhat higher than this work’s 7.76). SFRs of the host of GRB 060218 in the literature vary somewhat, with Wiersema et al. (2007) finding $0.065 M_\odot \text{ yr}^{-1}$, Sollerman et al. (2006) giving $\sim 0.05 M_\odot \text{ yr}^{-1}$, and Modjaz et al. (2008) finding $\sim 0.03 M_\odot \text{ yr}^{-1}$. The last of these values is comparable to the SFR found here when metallicity is not considered; no previous studies have accounted for the probable overestimation of SFR by classical diagnostics in low-metallicity galaxies.

Sokolov et al. (2001) found an $E(B - V)$ for the host of GRB 991028 of $0.51 - 0.60$. The extinction values presented here confirm that unlike many GRBs, GRB 991208 occurred in a rather dusty galaxy. Castro-Tirado et al. (2001) estimated the SFR of this galaxy to be $5 - 18 M_\odot \text{ yr}^{-1}$; this work narrows that range to $8 - 9 M_\odot \text{ yr}^{-1}$ if the galaxy has a high metallicity. If it falls on the lower metallicity branch, the SFR may be almost an order of magnitude lower.

4.2. Comparison to Field Galaxies

A key question surrounding GRBs is: do they occur primarily in low metallicity environments? Figure 3 shows the position of GRBs 060218 and 991208 relative to the local luminosity-metallicity relation of M. Bagley et al. (2008, in preparation). We adopt the absolute magnitudes of Savaglio et al. (2008), converted into the Johnson system: the host of GRB 060218 has $M_B = -15.97$, and the host of GRB 991208 has $M_B = -19.59$. For accurate comparison, all metallicities given are based on the Kewley & Dopita (2002, hereafter KD02) calibration. At low metallicities, this is an average of the M91 and KK04 oxygen abundances; at high metallicities, M91 and KK04 values

Table 2. Properties of Observed GRB Host Galaxies

Line	GRB 060218		GRB 991208	
$E(B - V)$	0.00	0.05	0.57	0.60
Metallicity ($12 + \log(\text{O}/\text{H})$)				
T_e	7.58	7.56
M91 Low	7.98	8.00	7.84	7.85
M91 High	8.73	8.72
KK04 Low	7.76	7.82	8.06	8.07
KK04 High	9.07	9.07
Star Formation Rate ($M_\odot \text{ yr}^{-1}$)				
$\text{H}\alpha^{\text{a}}$	0.0240 ± 0.0003	0.0269 ± 0.0003
$[\text{O II}]^{\text{a}}$	0.0293 ± 0.0090	0.0365 ± 0.0113	8.18 ± 0.37	9.33 ± 0.42
Low-Z $\text{H}\alpha - T_e^{\text{b}}$	0.0125 ± 0.0001	0.0141 ± 0.0001
Low-Z $\text{H}\alpha - R_{23}^{\text{b}}$	0.0119 ± 0.0001	0.0134 ± 0.0001
Low-Z $[\text{O II}]^{\text{c}}$	0.0055 ± 0.0001	0.0070 ± 0.0001	1.62 ± 0.058	1.86 ± 0.067

^aFrom the prescription of Kennicutt (1998).

^bFrom the prescription of Kewley et al. (2007).

^cFrom the prescription of Kewley et al. (2004).

are converted to the KK04 scale with the formulae of Kewley & Ellison (2008). Metallicities for both extremes of extinction for each galaxy are shown; these are the symbols slightly offset from each other. The three locations of GRB 991208 on the graph are its possible low metallicity and its M91 and KK04 high metallicities converted to the KD02 scale. The same relative metallicities are maintained when the local luminosity-metallicity relation is plotted using other oxygen abundance calibrations.

As Figure 3 shows, the host of GRB 060218 lies at a low metallicity but not one that is significantly offset from other galaxies of its luminosity. It is also comparable to the extremely metal-poor galaxies (XMPGs) of Kewley et al. (2007). Interpretation of the position of the host of GRB 991208 depends on whether it lies on the high- or low-metallicity branch. If it lies on the high-metallicity branch, it falls along the luminosity-metallicity relation; if on the lower-metallicity branch, it is very metal-poor for its luminosity, too much so to be accounted for by the evolution of the luminosity-metallicity relation with redshift. Average galaxy metallicity is lower by only ~ 0.15 dex at $z \sim 0.7$ versus $z \sim 0$ (Kobulnicky et al. 2003).

Adopting the low metallicity for the host of GRB 991208 would place this galaxy close in the luminosity-metallicity plane to some of the GRB hosts studied by Kewley et al. (2007). Determining whether the host of GRB 991028 has a high or low metallicity will be a key step in characterizing this galaxy and the GRB host population. High signal-to-noise near-infrared spectra, capturing the H α and [N II] emission lines, will help break the R_{23} -metallicity degeneracy.

The SFR of the host of GRB 060218 is equivalent to those of the XMPGs of Kewley et al. (2007), while the host of GRB 991208 has a much higher SFR than that sample. A useful comparison would be the specific star formation rate (SFR per unit mass), because the GRB 991028 host is brighter and therefore likely more massive than the XMPGs. The host galaxy of GRB 991028 is also dustier than the majority of GRB hosts (e.g., Savaglio et al. 2008).

In summary, although the sample size is as yet too small to conclude anything general about the properties of GRB hosts, the hosts of GRBs 060218 and 991208 illustrate the wide range of galaxies in which GRBs can occur. Their differences emphasize the need for more high-resolution optical and near-infrared spectra of GRB host galaxies.

This project was supported by funding from the National Science Foundation for the Research Experience for Undergraduates program at the Institute for Astronomy at the University of Hawai'i. The data presented herein were obtained at the W.M. Keck Observatory, which is operated as a scientific partnership among the California Institute of Technology, the University of California and the National Aeronautics and Space Administration. The Observatory was made possible by the generous financial support of the W.M. Keck Foundation. The authors wish to recognize and acknowledge the very significant cultural role and reverence that the summit of Mauna Kea has always had within the indigenous Hawaiian community. We are most fortunate to have the opportunity to conduct observations from this mountain.

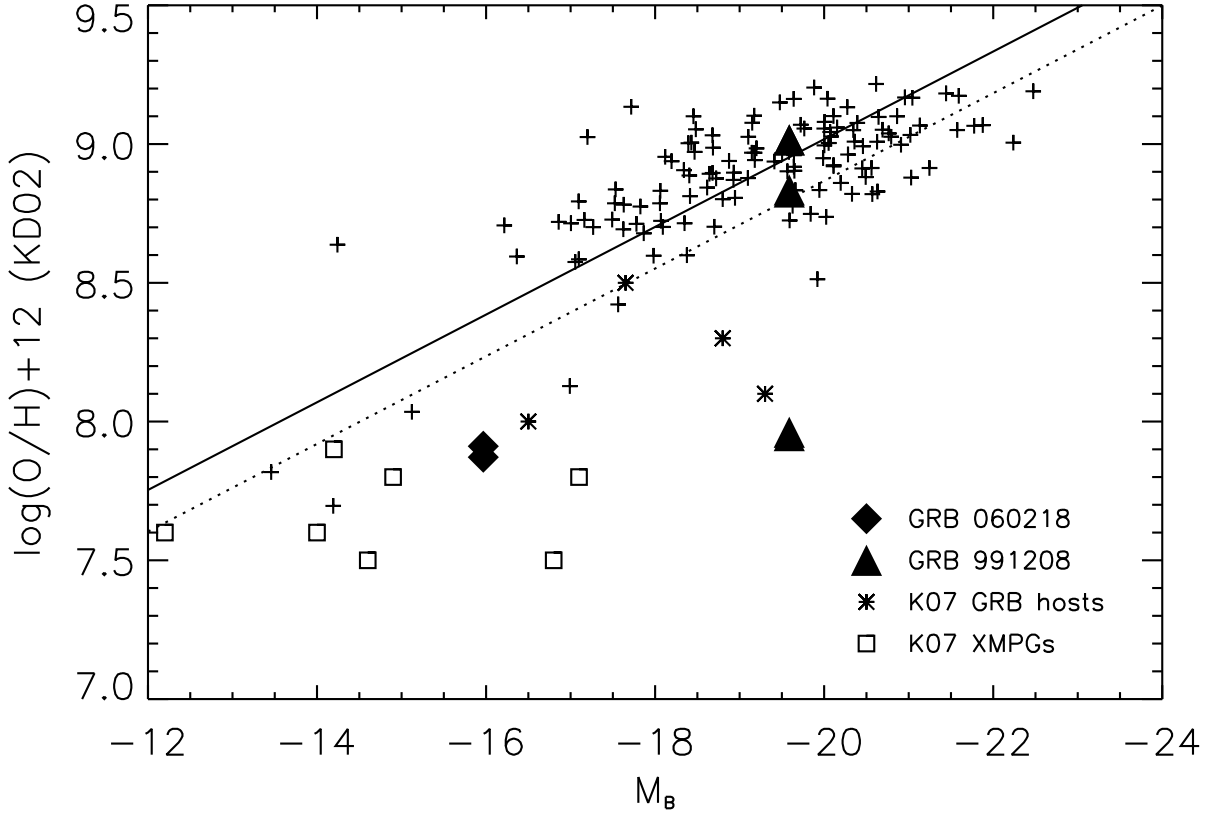


Fig. 3.— The hosts of GRBs 060218 and 991208 overplotted on the luminosity-metallicity relation of M. Bagley et al. (2008, in preparation). Both the high and low metallicities for GRB 991208 are plotted; the two sets of high metallicities come from two conversions into the Kewley & Dopita (2002) metallicity diagnostic. The two symbols slightly offset from each other at each GRB host metallicity are due to metallicities calculated at two different values of extinction for each galaxy. The solid line is the fit to the local galaxies; the dotted line is that fit shifted down by 0.15 dex to approximate the evolution of the luminosity-metallicity relation to $z \sim 0.7$. Also plotted are four GRB hosts and seven extremely metal-poor galaxies (XMPGs) from Kewley et al. (2007, K07 above).

REFERENCES

- Cardelli, J. A., Clayton, G. C., & Mathis, J. S. 1989, *ApJ*, 345, 245
- Castro-Tirado, A. J., et al. 2001, *A&A*, 370, 398
- Fruchter, A. S., et al. 2006, *Nature*, 441, 463
- Fynbo, J. P. U., et al. 2003, *A&A*. 406, L63
- Gehrels, N., et al. 2004, *ApJ*, 611, 1005
- Gorosabel, J., et al. 2005, *A&A*, 444, 711
- Izotov, Y. I., Stasińska, G., Meynet, G., Guseva, N. G., & Thuan, T. X. 2006, *A&A*, 448, 955
- Kennicutt, R. C., Jr. 1998, *ARA&A*, 36, 189
- Kewley, L. J., Brown, W. R., Geller, M. J., Kenyon, S. J., & Kurtz, M. J. 2007, *AJ*, 133, 882
- Kewley, L. J., & Dopita, M. A. 2002, *ApJS*, 142, 35
- Kewley, L. J., & Ellison, S. L. 2008, *ApJ*, 681, 1183
- Kewley, L. J., Geller, M. J., & Jansen, R. A. 2004, *AJ*, 127, 2002
- Kobulnicky, H. A., Kennicutt, R. C., Jr., & Pizagno, J. L. 1999, *ApJ*, 514, 544
- Kobulnicky, H. A., & Kewley, L. J. 2004, *ApJ*, 617, 240
- Kobulnicky, H. A., et al. 2003, *ApJ*, 599, 1006
- Kouveliotou, C., Meegan, C. A., Fishman, G. J., Bhat, N. P., Briggs, M. S., Koshut, T. M., Paciesas, W. S., & Pendleton, G. N. 1993, *ApJ*, 413, L101
- Le Floc'h, E., Charmandaris, V., Forrest, W. J., Mirabel, I. F., Armus, L., & Devost, D. 2006, *ApJ*, 642, 636
- Le Floc'h, E., et al. 2003, *A&A*, 400, 499
- McGaugh, S. S. 1991, *ApJ*, 300, 140
- Modjaz, M., et al. 2008, *AJ*, 135, 1136
- Osterbrock, D. E. 1989, *Astrophysics of Gaseous Nebulae and Active Galactic Nuclei* (Mill Valley: University Science Books)
- Pérez-Montero, E., & Díaz, A. I. 2003, *MNRAS*, 346, 105
- Pettini, M., & Pagel, B. E. J. 2004, *MNRAS*, 348, 59

- Savaglio, S., Glazebrook, K., & Le Borgne, D. 2008 [arXiv0803.2718S]
- Schaerer, D., & Vacca, W. D. 1998, *ApJ*, 497, 618
- Shaw, R. A., & Dufour, R. J. 1994, *Astronomical Data Analysis Software and Systems III*, ASP Conf. Ser., 61, 327
- Sokolov, V. V., et al. 2001, *A&A*, 372, 438
- Stanek, K. Z., et al. 2006, *Acta Astron.*, 56, 333
- Sollerman, J., et al. 2006, *A&A*, 454, 503
- Vink, J. S., & de Koter, A. 2005, *A&A*, 442, 587
- Wiersema, K., et al. 2007, *A&A*, 464, 529
- Woosley, S. E., & Bloom, J. S. 2006, *ARA&A*, 44, 507
- Woosley, S. E., & Heger, A. 2006, *ApJ*, 637, 914